THE AMERICAN SOCIETY OF MECHANICAL ENGINEERS
Three Park Avenue, New York, N.Y. 10016-5990

99-GT-65

FULL LOAD AND PART-LOAD PERFORMANCE PREDICTION FOR INTEGRATED SOFC AND MICROTURBINE SYSTEMS

Stefano Campanari
Research Assistant
Energetics Dept., Politecnico di Milano
Piazza Leonardo da Vinci 32, 20133 Milano - Italy
E-Mail: stefano.campanari@polimi.it

Abstract

During the last years, two new subjects among the others have risen interest in the field of small scale electric power generation: advanced microturbines and Solid Oxide Fuel Cells.

This paper investigates the thermodynamic potential of the integration of the Solid Oxide Fuel Cell technology with microturbine systems, in order to obtain ultra-high efficiency small capacity plants, generating electric power in the range of 250 kW with 65% LHV net electrical efficiency and with the possibility of cogenerating heat. A detailed description of the calculation model is presented, capable of full and part-load performances analysis of the microturbine and of the integrated SOFC+microturbine system.

Nomenclature

A_c	cell active area (cm^2)
$c_{p,0}$	specific heat at ambient temperature (kJ/(kg·K))
F	Faraday's constant (96439 Coulomb/mol of electrons)
i_c	cell current density (mA/cm^2)
m	mass flow rate (kg/s)
n	rotation speed (rpm)
p	pressure (Pa)
P_{el}	electric power (MW)
Q_{th}	thermal power (MW)
T	temperature (°C or K)
U_a	cell air utilization factor: $U_a=O_{2,consumed} / O_{2,inlet}$
U_f	cell fuel utilization factor: $U_f=(H_{2,consumed})/(H_{2,inlet}+CO_{inlet}+4CH_{4,inlet})$
V_c	cell voltage (V)
W_{el}	electric specific work (kJ/kg)
X_{O2}	oxygen molar fraction
β	pressure ratio
Δh	enthalpy change (kJ/kg)
ε_R	recuperator effectiveness
η	isentropic efficiency
η_p	polytropic efficiency
η_{el}	electric efficiency
η_{th}	thermal efficiency
ρ	density (kg/m^3)

Subscripts

c,t	compressor, turbine respectively
r	corrected conditions
re	real
ref	reference conditions (15°C, 101325 Pa)

Acronyms

DC/AC	direct / alternating current
FC	fuel cell
GT	gas turbine
LHV	lower heating value (kJ/kg)
SOFC	solid oxide fuel cell
TIT	turbine inlet temperature (total conditions)
TOT	turbine outlet temperature (total conditions)

1. INTRODUCTION

It is well known that recuperated microturbine units generating 50-200 kW are projected to achieve net electrical efficiencies approaching 30%(LHV), with low pressure ratios, uncooled operation and turbine inlet temperatures close to 900°C (Barker, 1997; De Biasi, 1998). Solid Oxide Fuel Cells (SOFCs) on their own achieve 50% net electrical efficiencies and have already been considered for integration with multi-MW gas turbine cycles, projected to achieve extremely high efficiencies for electric power production (Harvey and Richter, 1994; Stephenson and Ritchey, 1997; Lubelli and Massardo, 1998; Campanari and Macchi, 1998). The recent successful operation of a 100 kW SOFC plant (Veyo and Forbes, 1998), with direct natural gas feeding and internal reforming, offers the basis for considering small size plants, based on the successful integration of these two technologies, which could open new market spaces for the beginning of their commercialization (Campanari and Macchi, 1999).

The SOFC system exhaust temperatures (in the range of 800-900°C) are adequate for an exploitation in a microturbine with the above-mentioned characteristics, and no kind of difficulty has emerged for operating the SOFC system at the pressure required by a microturbine (Bessette and George,1996). It is therefore possible to design a small recuperative gas turbine cycle, where the combustor is "substituted" by a SOFC system, fed with preheated and compressed

Presented at the International Gas Turbine & Aeroengine Congress & Exhibition
Indianapolis, Indiana — June 7–June 10, 1999
This paper has been accepted for publication in the Transactions of the ASME
Discussion of it will be accepted at ASME Headquarters until September 30, 1999

air, and generating hot exhaust gases expanded by the gas turbine.

As the interest in such small power systems is not restricted to full load operation only, this paper deals with a full load and part-load performance prediction for this kind of plants.

In the first sectinn of the paper, a model for predicting the performances of a single-stage, high-speed radial-to-radial microturbine is discussed, with recuperative operation, absence of variable-inlet-guide-vanes systems (typically not used on this kind of turbomachines) and with variable speed optimization. Subsequently, the part-lnad modeling of the SOFC is discussed. In the second sectinn nf the paper an integrated SOFC and recuperative microturbine plant is proposed, with a detailed analysis of the fuel cell operating parameters and of the other components characteristics (pressure drops, efficiencies), together with their effects on the plant efficiency. The performances at full and part-lnad nf such a system are predicted, together with the influence nf the ambient temperature. Calculations are performed based on state-of-the-art performances of small turbomachinery and on the most advanced SOFC tubular technology, with natural gas feeding, internal reforming of hydrocarbons and internal air preheating.

2. CALCULATION MODEL

2.1 The microturbine model; part-load operation

The developed model makes reference to a single stage gas turbine, with radial compressor and radial turbine and with a recuperative cycle arrangement. With an inlet mass flow rate of 0.4÷1.0 kg/s this model is representative for the 40÷80 kW-class microturbines actually developed by many manufacturers (De Biasi, 1998; Barker, 1997): as an example General Electric - Elliott Energy Systems distributes a 45 kW and an 80 kW recuperated gas turbine, with a pressure ratio of 4:1 and net electrical LHV efficiency of 30%, rated with a design speed of 116,000 and 68,000 rpm respectively and with a 0.41+0.84 kg/s mass flow rate (Anon., 1998); Allied Signal Aerospace Co. manufactures a 50 kW engine for vehicle applications with β=3.3 at 75,000 rpm (O'Brien, 1998) and a 75 kW genset with a pressure ratin of 3.8:1 and a design speed of approximately 85,000 rpm.

The high rotating speed of these compact machines require a rectifier+inverter power control system, flattening the high frequency AC output of the high speed generator and subsequently generating the requested grid frequency from the rectified direct current. It is interesting to note that this kind of process could be suitable for integration with the power conditioning system of a fuel cell, typically generating an AC output starting from the cell DC electrical generation.

The model adopts as a reference the compressor map given by Uchida et al. (1994) for a centrifugal compressor developed and tested for application in a 100 kW gas turbine, elaborated according to the similarity rules. This map shows an isentropic efficiency of about 79.5% at the manufacturer design point, which is rated at a pressure ratio of 5.0, 0.445 kg/s and 100,000 rpm, and values somewhat higher (80+82%) at lower speed. For the application discussed here, the design point has been set tn a pressure ratio of 3.8 and a specific speed of 0.13 (85,000 rpm at 0.5 kg/s): the resulting operating point, together with the partial load operating curve, is shown in Fig.1. The maximum efficiency was set to 79.5% at the design point, with a surge margin (in terms of mass flow) nf about 15%.

The curves are adimensionalized with respect to the design conditions, and recalculated in terms of corrected enthalpy change (instead of pressure ratio), corrected flnw rate and corrected speed, defined as following (with T, p, m_C at the compressor inlet):

$$\Delta h_r = \frac{\Delta h_{re}}{c_{p,0} T_{ref}} \tag{1}$$

$$m_r = m_C \frac{\sqrt{T/T_{ref}}}{p/p_{ref}} \tag{2}$$

$$n_r = \frac{n}{\sqrt{T/T_{ref}}} . \tag{3}$$

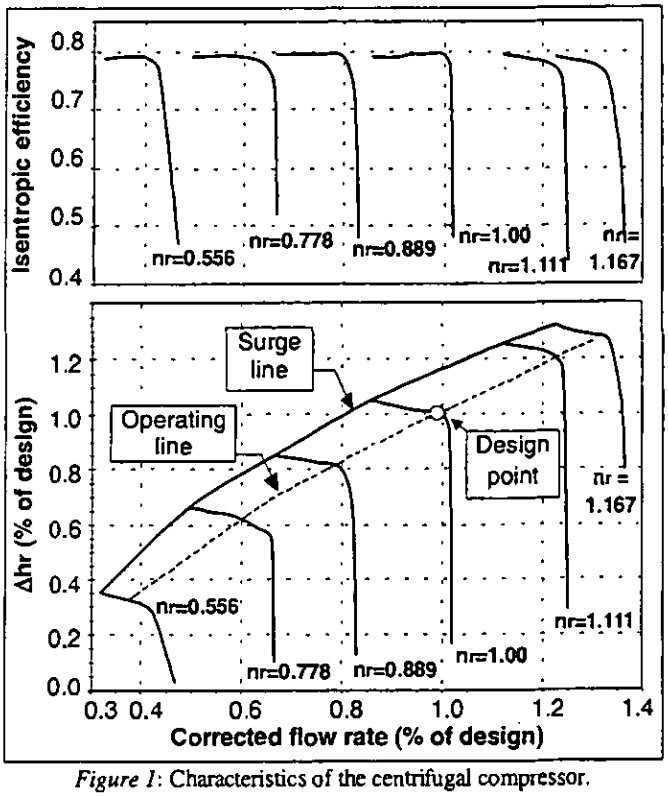

Figure 1: Characteristics of the centrifugal compressor.

Besides, the model includes a turbine map based on the works of Pullen et al. (1992) for a high pressure ratio radial inflow uncooled turbine, suitable with necessary scaling for engines in the 50–300 kW range. The design point for the turbine, tested and developed for power generation purposes and for small aircraft application, was originally set at a mass flow rate of 0.387 kg/s, 100,000 rpm, TIT=1200 K, total-to-static pressure ratio of 4.7 and total-to-static efficiency of about 82%.

For the application of this work it is considered to operate with the curves illustrated in Fig. 2, derived with appropriate scaling from the original map and recalculated as above in terms nf corrected quantities (with T, p, m_T at the turbine inlet); all the values are then adimensionalized with respect to the design conditions chosen here, which is characterized by a pressure ratio of 3.4, a specific speed of 0.11 (85,000 rpm at 0.5 kg/s) and a 0.82 total to static efficiency. The turbine is assumed to gain 2.5% with the diffuser recovery of the exhaust gas kinetic energy at the nominal point; at partial load the efficiency gain is reduced as the square of the flow rate.

The resulting design point turbine isentropic efficiency is therefore 84.5%. These values are in good agreement with the works of Jones (1994) and Kim et al. (1998) on microturbine development.

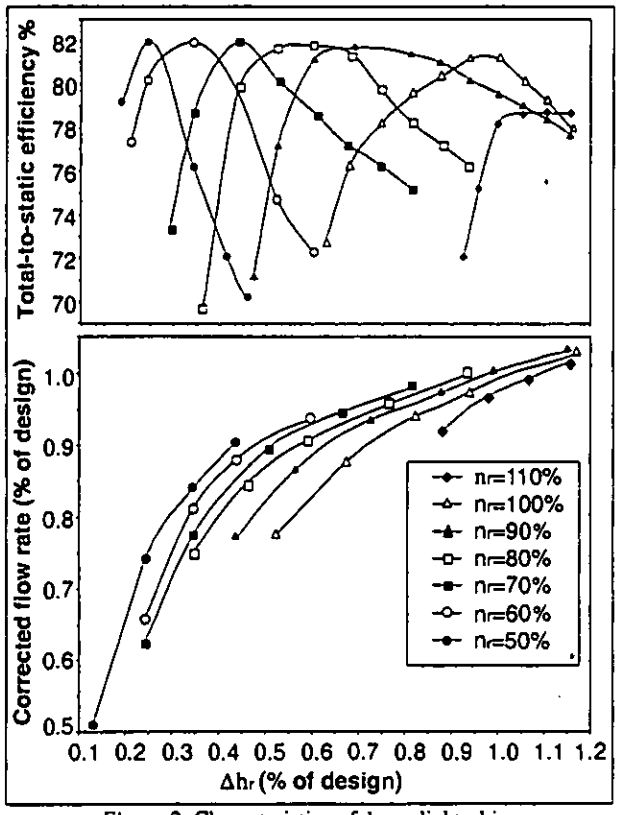

Figure 2: Characteristics of the radial turbine.

The other assumptions for the GT cycle calculation are shown in Tab. 1. The minimum temperature difference on the recuperator is set to 45°C; partial load calculation are made by keeping the heat exchanger area as a constant and assuming a dependence of the global heat transfer coefficient on the Reynolds number elevated by 0.6. According to these assumption, the resulting minimum temperature difference becomes lower when the thermal duty of the heat exchanger is reduced.

Pressure ratio (design point)	3.8
Combustor outlet temperature (design point)	900 °C
Recuperator Δp/p air/gas side (design point)	3% / 6%
Minimum ΔT recuperator (design point)	45°C
Heat loss recuperator (design point; T_{amb}=15°C)	2%
Combustor Δp/p	6%
Combustion efficiency	98.5%
Organic efficiency (design point)	96%
Electric generator efficiency (design point)	95%
Power control system efficiency (design point)	96%
Fuel compressor efficiency	70%
Fuel (natural gas) composition: CH_4 98% - C_2H_6 0.7% - C_3H_8+C_4H_{10} 0.3% - Sulfur compounds 50 ppmv - N_2 1%	

Table 1: Gas turbine cycle model assumptions.

The air and gas side pressure drops are set to 3% and 6% respectively at design conditions (accounting for different density and gas speed), and they are varied at partial load as a function of the mass flow and density according to the following relation:

$$\Delta P \cong \text{Const} \times \frac{m^2}{\rho} \qquad (4)$$

as by the Darcy equation for turbulent flows, assuming a negligible variation of the friction factor.

The total amount of the recuperator heat loss is kept constant and independent with respect to the load, assuming that it is mostly influenced by the external temperature of the insulation, which is almost constant at partial loads. The same applies for the SOFC heat losses. The combustor pressure drop is kept for simplicity constant at partial load.

The combustor outlet temperature is set to 900°C, even if some manufacturers declare higher values, close to 1000°C (O'Brien, 1998; Holbrook, 1998). The resulting design point configuration is shown in Fig. 3, with an LHV net electrical efficiency of about 30% and a 55.2 kW output.

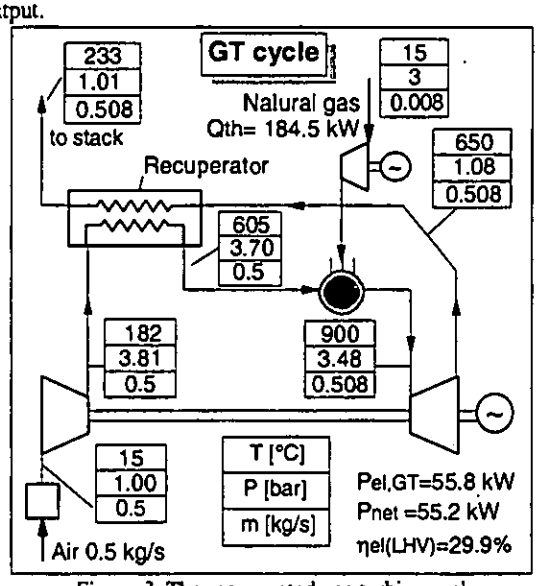

Figure 3: The recuperated gas turbine cycle.

The electrical generator efficiency, together with the power conditioning (rectifier and inverter) system efficiency and the gas turbine organic efficiency are reduced at partial load as shown in Fig. 4. The organic efficiency curve is generated assuming that the design point loss amount is constant at partial load. The generator design efficiency of 95% is consistent with latest prototype test results (Carnö et al.,1998). The inverter system efficiency has been set to 96% (Ray and Ruby, 1992), a value lower than the maximum efficiency (97%) quoted by some manufacturer (Fimet, 1998); an efficiency decay of about 5% at 10% load was assumed to quantify the effects of auxiliary losses (ventilation etc.), of main bridge and thyristors losses, etc.

The combustion efficiency is set to the conservative value of 98.5%, while even 99.5% appears to be feasible (O'Brien, 1998).

The operation at reduced power can be made:

- by a reduction of fuel flow and TIT at constant speed: the operating point on the compressor curve is moved to the right, and the pressure ratio is reduced to accommodate the mass flow requested by the turbine. The operating point on the turbine curves move towards lower TITs, higher n_r (eq. 3) , lower Δh_r (or pressure ratio) and m_r. The compressor/turbine matching requires a working condition characterized by a little increase in the air mass flow, a reduction of the turbine and compressor efficiency and great penalties on the cycle efficiency.
- by a reduction of speed at constant TIT (or with a moderate reduction of TIT): the new operating point for the compressor follow the dashed curve in Fig. 1, resulting in a lower pressure ratio and a corrected mass flow on the turbine compatible with the requested TIT. The operating point on the turbine curves move towards lower n_r and lower Δh_r. The new working condition is characterized by high compressor and turbine polytropic efficiency and yields almost constant cycle efficiency; the compressor surge margin is always kept around 15%.

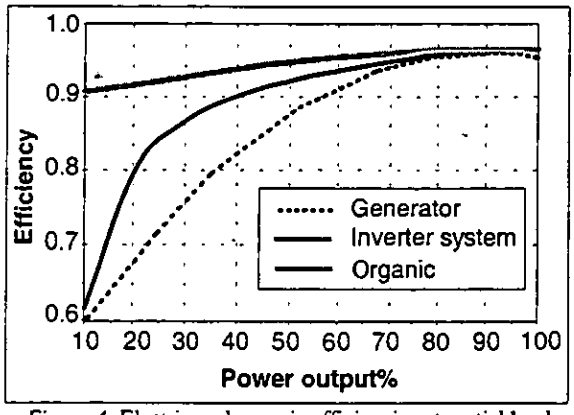

Figure 4: Electric and organic efficiencies at partial load.

The results of these calculations are presented in Fig. 5. It is possible to note that the variable speed operation with constant TIT, or with small TIT reduction, should give the best partial load performances for this machine. At 50% of the full power output it is than possible to achieve a still very high system efficiency, just about 3 percentage points lower than the design efficiency. This is possible because:

1) the sensible mass flow reduction leads to reduced pressure losses;

2) the reduced duty on the recuperator leads to a higher heat exchange effectiveness (Fig. 6), ranging from about 89% to over 93% at the lower loads;

3) the compressor and turbine efficiencies are still high, and the turbomachines are still working in a near-optimum zone (Fig. 6): the isentropic efficiency variation is below 5% at about 60% speed.

The circumstance that the cycle efficiency remains high at very low pressure ratios is however typical of recuperative gas turbine cycles. Without considering the electrical losses, the gross efficiency map (here not represented) would show also an expected reduction of the optimum pressure ratio at lower turbine inlet temperatures.

The recuperator effectiveness has a relatively high value (≈89%) at design conditions, whose effects on the plant economics are not discussed here; a similar value is reported by Camö et al. (1998).

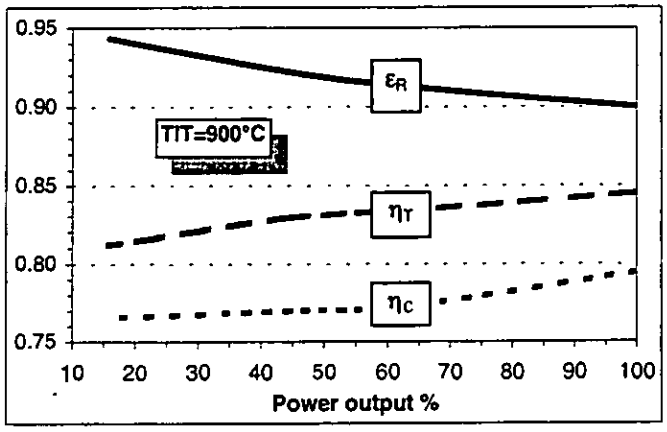

Figure 6: Compressor and turbine isentropic efficiencies and recuperator effectiveness for the gas turbine cycle at partial load (constant TIT operation).

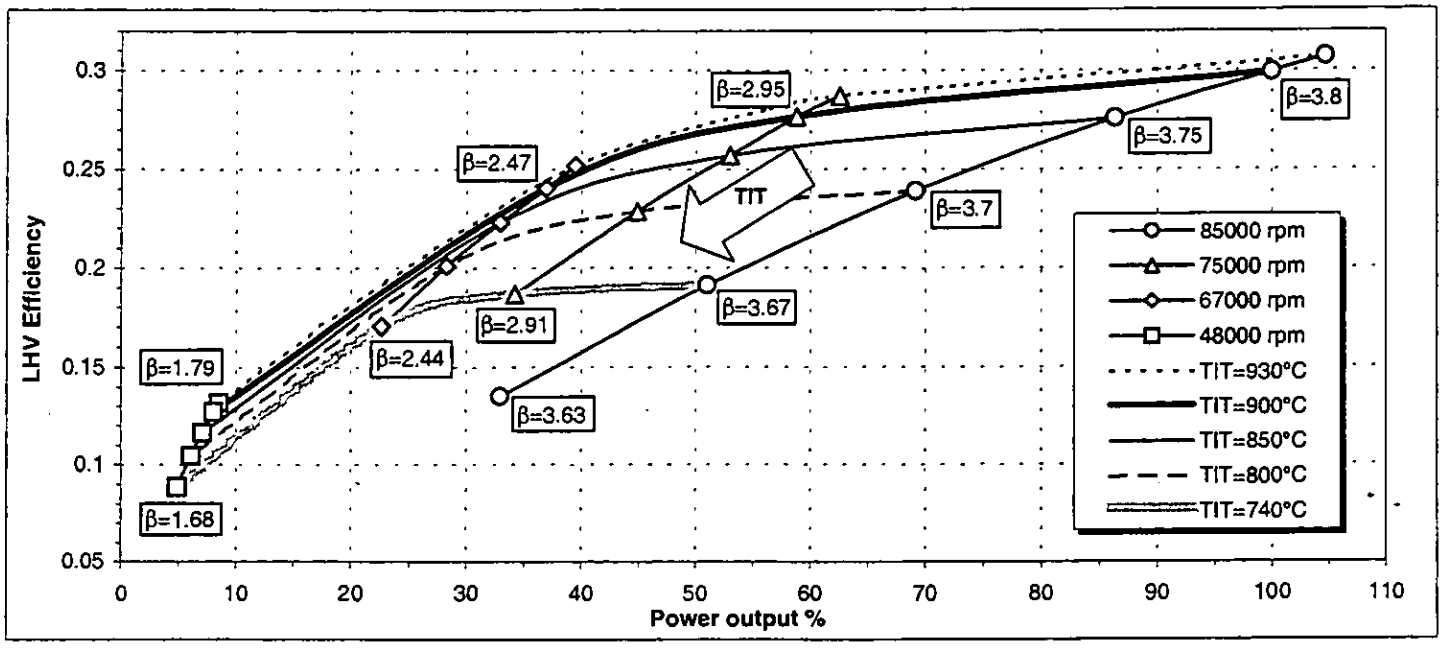

Figure 5: Calculated gas turbine performances at partial load.

2.2 The SOFC Model; part-load operation

It is made reference to the latest generation of the tubular SOFC, the Westinghouse Air Electrode Supported (AES) fuel cell, with operating temperature of 1000°C, which has been recently tested up to a 100 kW plant size, with the possibility of being easily upgraded to about 200 kW output (Singhal,1997; Veyo and Forbes,1998).

The SOFC is fed by an oxidizer (air) and a fuel. The two fluxes flow in contact with cathode and anode porous surfaces, separated by a solid electrolyte which is a good $O^=$ ion-conductor at the high SOFC operatiog temperatures. The reduction of molecular oxygen to $O^=$ takes place at the cathode, while the fuel is oxidized to steam and carbon dioxide at the anode. The prevailing oxidization reaction is the hydrogen consumption. Hydrogen is generated by internal steam reforming and water-gas shift reactions starting from the natural gas feeding and exploiting the fuel cell high-temperature heat production. Steam is obtained by recirculating a fraction of the anode exhaust gases. The SOFC model is based on these reactions (Hirschen-

hofer,1994); however the high temperature SOFCs sustain also a fraction of CO and CH_4 direct oxidization. The Westinghouse tubular SOFC system operates following these principles; it is provided with anode recirculation, sustained by an ejector using fresh fuel as driving flow, and with a small pre-reforming step cracking the higher hydrocarbons and reducing carbon deposition problems. The exhaust air and fuel flow, partially consumed by the cell, react up to complete fuel oxidization with an auxiliary combustion; the high temperature gases preheat the inlet air flow before being delivered to external components (Ray and Ruby, 1992, Veyo, 1996). The alternative of external reforming, often considered for planar SOFC feeding, is not discussed here, as it is not employed by the most advanced tubular technology and it adds complexity to the plant configuration.

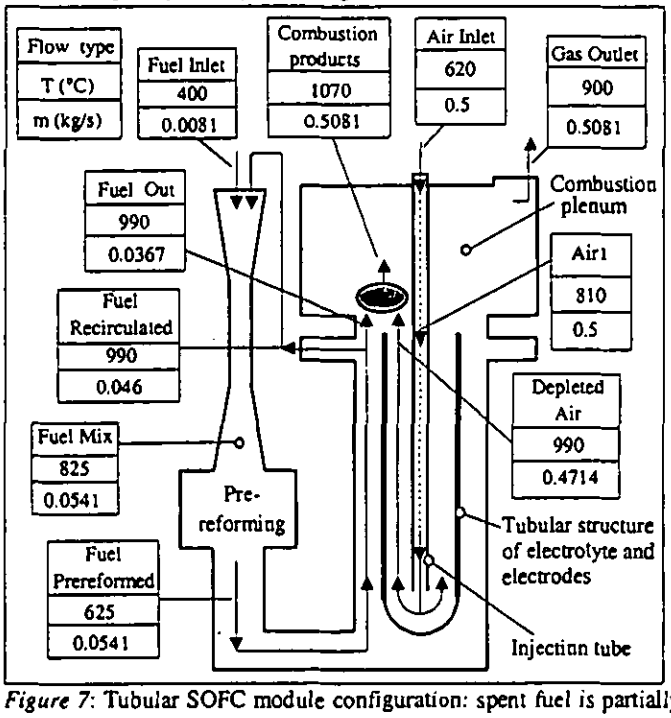

Figure 7: Tubular SOFC module configuration: spent fuel is partially recirculated and the exhaust gases of the auxiliary combustion are used to preheat the inlet air flow.

The FC generates direct current electrical energy with an efficiency proportional to its voltage (Bessette and George,1997; Hirschenhofer et al.,1994). Fuel and air are not completely consumed at the electrodes to avoid the large voltage losses due to reactant concentration gradients and limited gas diffusivity near the electrodes active area; air and fuel utilization factors (see nomenclature) quantify the consumed fraction.

The SOFC schematic is shown in Fig. 7. The fuel is desulfurized natural gas, internally reformed by the SOFC itself; the fuel pressure is calculated to ensure the ejector operation. An external compressor rises the natural gas pressure from the 0.3 MPa available in any small network up to the requested pressure (i.e. 1 MPa). Other details about the cell model are discussed in Campanari and Macchi (1997 and 1998). The fuel cell efficiency is positively affected by pressurized operation, with an increase proportional to the operating pressure, while the efficiency decreases by increasing the cell current density.

The model calculates the cell electric power production, heat generation and efficiency together with the thermodynamic properties and chemical composition of internal and external flows in all the representative points, as a function of the cell operating conditions (temperature, pressure, current density, fuel and oxidizer composition and utilization factors).

The cell power output is given by:

$$P=V\times I=V_c\times i_c\times A_c \qquad (5)$$

where i_c is the cell current density and A_c the cell active area. The equation shows that a reduction of the FC power output requires a reduction of the cell current density[1].

In order to define the possible techniques for part-load operation of an integrated SOFC+GT plant, it is necessary to discuss the mutual dependence of the involved variables, which are the cell current density, the air utilization factor and the cell module exhaust temperature.

The temperature of the compressed air fed to the fuel cell module is generally in the range 500÷700°C; the air flow is then preheated by the cell exhaust up to the temperatures required for the cell cooling (point "Air1" in Fig. 7). It should be noted that the calculation model considers that the depleted air temperature at the cathode outlet is almost constant (close to 1000°C), and that the temperature at the Air1 point of Fig. 7 follows the cell heat generation, with maximum variations of 50-100°C; the effective air temperature at the cell electrodes inlet (end of the injection tube) is by this way always close to 900°C, high enough to allow the solid electrolyte operation.

The cell air utilization can be expressed as:

$$U_a=\frac{m_{O_2,consumed}\,(mol/s)}{m_{O_2,inlet}\,(mol/s)}=\frac{1}{X_{O_2}\,m_{air,inlet}\,(mol/s)}\cdot\frac{i_c\cdot A_c}{4F} \qquad (6)$$

where F is the Faraday's constant (see nomenclature).

Any change of the air utilization factor at constant air flow will yield a variation of the cell exhaust temperature, as the cell heat generation is mainly discharged to the air flow (the remaining being partly taken by the fuel flow and partly lost to the ambient): lowering U_a will cause a reduction of the cell module exhaust temperature.

With these hypothesis the SOFC exhaust temperature is calculated as a function of the air/fuel inlet temperature, the air/fuel utilization factors and the cell voltage and efficiency. This model gives the possibility of predicting part-load operating conditions and performances.

Two different techniques for cell power reduction (part-load operation) have therefore been considered:

- Constant air flow - Starting from a design point condition, it is possible to reduce the cell current density with a constant air flow, lowering also the air utilization factor (eq. 6) with a linear proportion, and reducing the FC power output.

A reduction of i_c and U_a will result in a certain increase of the cell voltage V_c calculated by the model (due to a reduction of resistance and cell polarization losses, as well as to the higher average oxygen concentration in the air flow), with a global efficiency gain parallel to the power output reduction. The effect of a reduction of U_a is also a reduction of the cell exhaust temperature. This first kind of power reduction is suitable for matching the gas turbine operation at constant speed, almost constant air flow and reduced TIT.

- Constant U_a - By this modality of part load operation, starting from a design point the air mass flow is progressively lowered. By lowering also the cell current density it is possible to keep the same air utilization (eq. 6). This would give the same cell exhaust temperature, provided that the cell air inlet temperature is kept constant. However, the gas turbine at reduced speed and mass flow operates with a lower pressure ratio and higher TOT (with constant TIT), delivering hotter

[1] Another possibility, here not discussed further, is to reduce A_c with a by-pass system which excludes some of the cells during part-load operation; the system would be complicated by the necessity of keeping those cells at an adequate hot-stand-by temperature.

gases to the recuperator and hotter air to the FC inlet. It is therefore necessary to reduce furthermore the cell current density in order to keep the same cell exhaust temperature at U_a constant. By this practice, the TIT can be kept to the desired values; the large reduction of i_c will also significantly increase the cell voltage and efficiency. This modality of part-load operation is therefore suitable for matching the gas turbine operation at reduced speed, reduced mass flow and constant TIT.

The main assumptions in the SOFC model are shown in Tab. 2; the calculated reference cell voltage is 0.7 V at design conditions. In order to avoid to overestimate the cell efficiency at low loads, the maximum cell voltage has been set to the value corresponding to 100 mA/cm^2 (minimum value of i_c in Fig. 9).

The same considerations discussed for the efficiency of the gas turbine inverter system apply to the fuel cell DC/AC conversion. Natural gas is preheated at about 400°C to obtain the best efficiency in H_2S and sulfur compounds (mercaptans, odorizing substances) adsorption by mean of catalytic Zinc-Oxide beds; the H_2S concentration must be kept under 0.1 ppmv to avoid any cell degradation effect, even if 1 ppmv gives a limited and recoverable voltage reduction (Ray and Ruby,1992; Lundberg.1990).

Δp/p air/fuel side (design point)	5% / 2%
Δp/p auxiliary combustion	6%
Heat loss SOFC (design point; T_{amb}=15°C)	2%
Combustion efficiency	98.5%
DC-AC efficiency (design point)	96%
Fuel inlet temperature	400°C
Fuel utilization factor (single passage)	80%
Air utilization factor (design point)	25%
Current density (design point)	350 mA/cm^2
Steam-to-carbon ratio for recirculation	1.8
Fuel composition	as by Tab.1
Available fuel pressure	3 bar
Δp/p fuel preheater hot/cold side	2%
Fuel preheater min. ΔT	45°C

Table 2: SOFC model assumptions.

The air and fuel pressure losses are changed with mass flow and density as described by eq. 4. The SOFC total heat loss amount resulting from design point calculation (which includes the auxiliary combustion heat loss) is kept constant and independent of the load; the auxiliary combustion pressure loss percentage is also kept constant at part-load.

3. PLANT CONFIGURATION AND THERMODYNAMIC RESULTS

The proposed plant configuration is represented in Fig. 8 with the corresponding energy balances and with the thermodynamic conditions of all the relevant cycle points. It is basically a recuperative gas turbine cycle, where the SOFC receives the preheated and compressed air and delivers hot exhaust gases to the turbine. The main differences with respect to the original microturbine plant of Fig. 3 are the following:

- the pressure losses are larger: before reaching the gas turbine, the air flow passes through the recuperator, the SOFC and the auxiliary combustion process, with a total pressure drop of about 14% (vs. 9% for the GT cycle). The gas turbine operates therefore with a lower pressure ratio and a lower power output;
- the SOFC fuel flow is larger than the GT combustor fuel flow, thereby increasing the mass flow in the gas turbine;
- a fraction (about 3%) of the turbine exhaust flow is used to preheat the pressurized natural gas before the desulfurization process, up to about 400°C; hence the thermal capacity of the hot flow in the recuperator is a little lower;
- the conventional combustor is absent: this leads to substantial advantages for NO_x and CO emission abatement.

The analysis of SOFC+GT based power cycles is made with a simulation code already described in Campanari and Macchi (1998) and Consonni et al. (1991). The SOFC+GT performances were calculated in two steps: 1) the GT part load model discussed in 2.1 was used to calculate all the cycle parameters and component performances of the recuperative GT cycle; 2) the same operating conditions (GT pressure ratio and inlet/outlet temperatures, heat exchangers pressure drops etc., taking into account the design point parameters of Tab. 2) were used as input for the SOFC+GT model, providing point-by-point the corresponding performances of the SOFC+GT cycle.

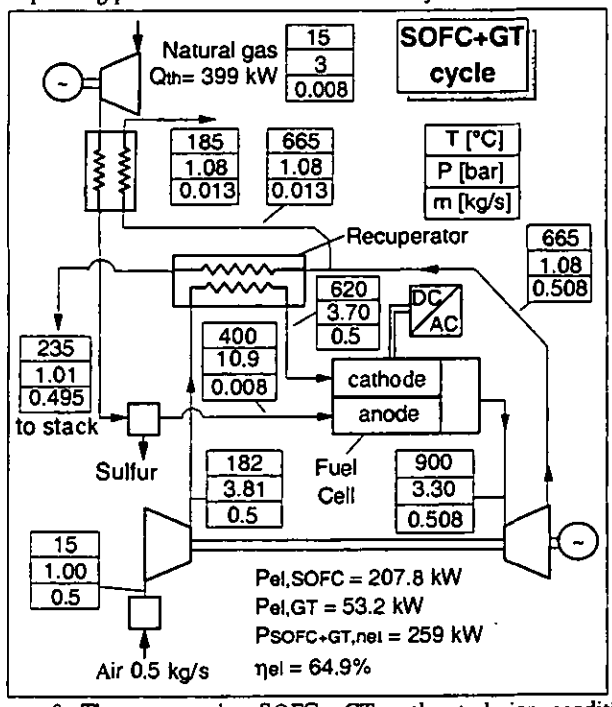

Figure 8: The recuperative SOFC+ GT cycle at design conditions; components assumptions as from Tab. 1 and 2.

Previous works have shown the possibility of obtaining net electrical efficiencies up to 75% (LHV) for medium (5-50 MW) or large scale (>100MW) power plants adopting advanced gas turbines and SOFC systems with configurations similar or more complex than the cycle represented in Fig 8: these plants benefit of both advanced GT cycles (intercooled, regenerative, reheated cycles) and the advantage of adopting high efficiency turbomachines (Stephenson and Ritchey,1997), often with the addition of complex heat recovery bottoming cycles (Bevc et al.,1996; Campanari and Macchi, 1998, Lobachyov and Richter, 1996).

The thermodynamic performances of the smaller size and simpler cycle proposed here are nevertheless really remarkable: the net LHV efficiency reaches 65% with a total power output of about 250 kW, generated with a 4:1 ratio respectively by the SOFC and the gas turbine; exhaust gases leave the plant at about 230 °C, giving the possibility of recuperating useful heat for cogeneration (see Tab. 4). These results confirm the possibility of obtaining high efficiencies with low pressure ratio SOFC and recuperated gas turbine cycles already investigated in a previous work (Campanari and Macchi,1998).

The reversible work losses of this cycle, are represented in Tab. 3

and compared to the GT cycle losses. The irreversibilities occurring in the fuel cell include power conditioning, heat exchange, auxiliary combustion and heat losses, and pressure drop losses. It is possible to note that: (i) the SOFC losses are about 15 points lower than the combustion losses occurring in the GT cycle; the large combustion loss is absent in the SOFC+GT cycle (the auxiliary combustion process loss weights for only one fourth of the total SOFC losses);

II law efficiency loss (%)	SOFC+GT	GT
SOFC	18.5	-
Combustor GT (including ΔP, η_{th})	0	33.0
Compressor (including ΔP air filter)	2.9	6.2
Gas Turbine	2.0	4.4
Recuperator (ΔT,Δp,η_{th})	3.5	7.3
Other heat exchangers (ΔT,Δp,η_{th}, mix)	0.3	-
Aux, organic, electric GT and fuel compressor	2.0	4.3
Stack (exhaust gas)	7.7	15.6
η_{II} total	63.1	29.2

Table 3: Second law losses for the GT cycle and for the plant configuration of Fig. 8.

(ii) the losses related to compressor, turbine, recuperator and stack in the GT cycle are more than double with respect to the SOFC+GT cycle: this happens because in the SOFC plant the majority of the plant electric power is generated by the fuel cell, and the resulting higher fuel input reduces the weight of the losses related to the gas turbine section.

Plant characteristics	SOFC+GT	GT
Fuel flow in × LHV (kW)	399	185
Air flow at filter inlet (kg/s)	0.5	0.5
Combustor / FC outlet temperature (°C)	900	900
SOFC system power (kW)	209	-
GT power (kW)	53.5	56
Auxiliary power (kW)	3.0	0.5
Net total power (kW)	259.5	55.5
T exhaust (°C)	235	235
Turbine exhaust temperature (°C)	665	650
η_{el} (LHV)	64.9%	29.9%
Thermal power of exhaust gases(*) (kW)	83	83
I law efficiency with cogeneration(*)	86%	76%

Table 4: SOFC+GT and GT plant characteristics; (*)T stack = 75°C.

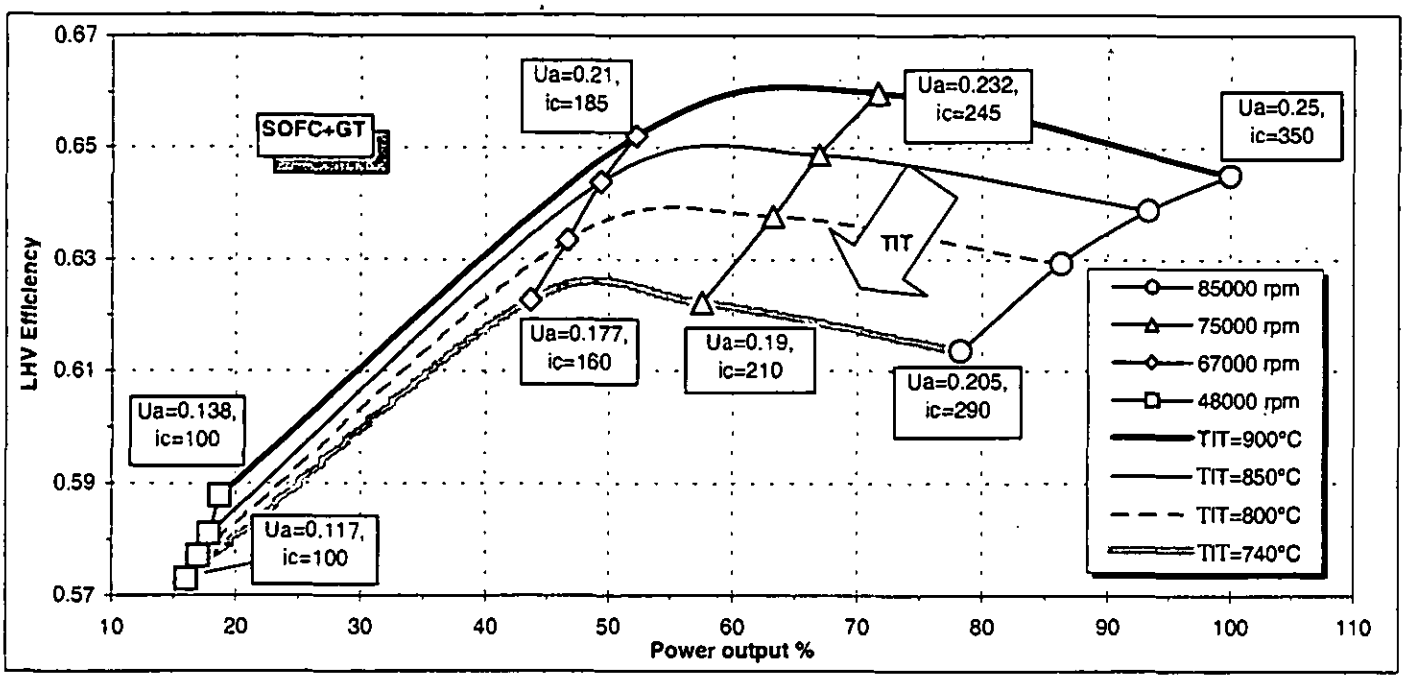

Figure 9: Partial load performances of the SOFC+GT cycle. The cell current density is reduced according to eq. 5, with lower limit at 100 mA/cm^2.

Figure 9 shows the results of the SOFC+GT cycle calculations at partial load: it is interesting to note how the fuel cell capability of achieving higher efficiencies at partial load is reflected on the total system efficiency, raised of about 3 percentage points at 60% of the full power output. The power distribution between the fuel cell and the gas turbine is shown in Fig. 10: at reduced output the fuel cell weight increases, raising up to more than 6:1 the power ratio with the gas turbine; by this way, thanks to the FC inherent performance gain, the system attains still a high electric efficiency. The heat production associated with the exhaust gases is almost linearly reduced at lower power outputs, with a little reduction of the exhaust temperature due to the lower compressor pressure ratio and to the more effective gas cooling in the recuperator.

Figure 11 deals with the calculated effects of changing the ambient temperature on the cycle performances; at nominal rpm, the surge margin decreases at lower temperatures, but it remains always over 12%.

5. CONCLUSIONS

Detailed calculations for the integration of SOFC and microturbine lead to a 250 kW-class plant with 65% net electrical efficiency (LHV). The possibility of demonstrating such performances on such a small scale plant, based on the available and existing 100 kW-class SOFC technology, could open wide and interesting markets for the future commercialization of these technologies.

The partial load analysis carried out in this paper demonstrates the possibility of obtaining very high system electric efficiency even at reduced plant electrical output, exploiting the fuel cell characteristical performance improvement at low current densities and microturbine

variable-speed optimization. The energy-savings deriving by the application of such a system to cogeneration on small capacity plants are discussed in Campanari and Macchi (1999).

6. ACKNOWLEDGMENTS

The reported research was conducted at the Energetics Department of Politecnico di Milano as a part of the author's doctoral research under the supervision of Professor Ennio Macchi. The author thanks him for his guidance and constant support.

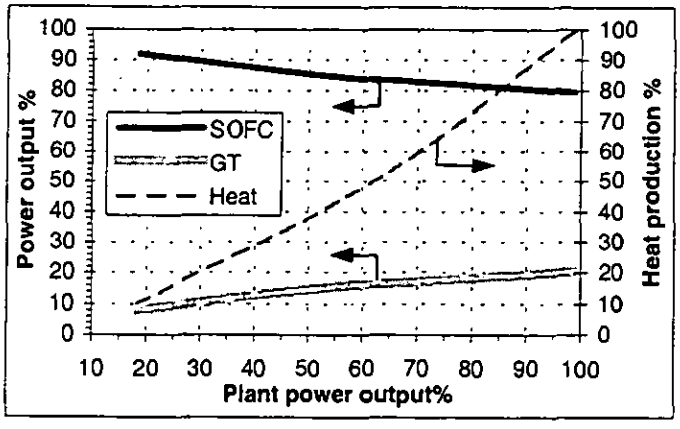

Figure 10: SOFC+GT plant power distribution and heat production as a function of the load, for constant TIT operation.

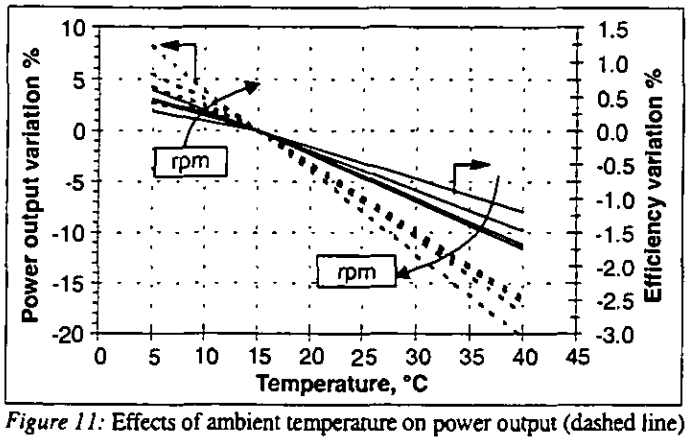

Figure 11: Effects of ambient temperature on power output (dashed line) and cycle efficiency (solid line); the TIT is set to 900°C and each group of four lines is traced for 48000, 67000, 75000 and 85000 rpm.

REFERENCES

Anon. (1998) "Elliott energy systems – The TA series turbo alternator®", preliminary specifications of TA turbogenerators, Elliott energy systems Inc., Stuart, Florida.

Barker T. (1997) (editor) "Power-gen international '96: micros, catalysts and electronics", Turbomachinery International, Vol.38, No.1, pp. 19-21, January/February 1997.

Bessette N.F., George R.A.(1996) "Electrical performance of Westinghouse's AES solid oxide fuel cell", 2nd International Fuel Cell Conference, (IFCC 4-12) Japan, 1996.

Bevc F.P., Lundberg W.L., Bachovchin D.M. (1996) "Solid Oxide Fuel Cell combined cycles", ASME 96-GT-447.

Carnö J., Cavani A., Liinanki L. (1998) "Micro gas turbine for combined heat and power in distributed generation", ASME paper 98-GT-309.

Campanari S., Macchi E. (1997) "Integrated cycles with solid oxide fuel cells and gas-steam combined cycles" (in Italian), IX congress Technologies and Complex Energy Systems "Sergio Stecco", Milano, June 1997.

Campanari S., Macchi E. (1998) "Thermodynamic analysis of advanced power cycles based upon solid oxide fuel cells, gas turbines and rankine bottoming cycles", ASME paper 98-GT-585.

Campanari S. , Macchi E. (1999) "The combination of SOFC and microturbine for civil and industrial cogeneration", accepted for publication at ASME Turbo Expo 1999, Indianapolis, USA.

Consonni S., Lozza G., Macchi E., Chiesa P., Bombarda P. (1991) "Gas-turbine-based advanced cycles for power generation - part A: calculation model" International Gas Turbine Conference-Yokohama 1991, Vol. III pp. 201-210, 1991.

De Biasi V. (1998) "Low cost and high efficiency make 30 to 80 kW microturbines attractive", Gas turbine world, Pequot Publishing Inc., No. 1-1998.

Fimet (1998) "Sinuson KT-series inverter losses", personal communications with Fimet Motori & Riduttori Co., Italy, 1998.

Harvey S.P., Ritcher H.J (1994) "Gas turbine cycles with solid oxide fuel cells – part I and II", Journal of energy resources technology, Vol.116, Dec. 1994.

Hirschenhofer J.H., Stauffer D.B., Engleman R.R. (1994) "Fuel cells, a handbook (Rev.3)", Gilbert/ Commonwealth Inc. for U.S. Department of Energy (DOE), 1994.

Holbrook J.D. (1998) personal communications with Elliott Energy Systems Inc., 1998.

Jones A.C. (1994) "Design and test of a small, high pressure ratio radial turbine", ASME paper 94-GT-135.

Kim S.Y., Park M.R., Cho S.Y. (1998) "Performance analysis of a 50 kW turbogenerator gas turbine engine", ASME paper 98-GT-209.

Lobachyov K., Richter H.J. (1996), "Combined cycle gas turbine power plant with coal gasification and solid oxide fuel cell", Journal of Energy Resources technology, Vol.118, Dec.1996.

Lundberg W.L. (1990) "System applications of tubular solid oxide fuel cells", proc. of the 25th IECEC pp.218-223, 1990.

Massardo A.F., Lubelli F. (1998) "Internal reforming solid oxide fuel cell-gas turbine combined cycles (IRSOFC-GT) – Part A: cell model and cycle thermodynamic analysis", ASME paper 98-GT-577.

O'Brien P. (1998) "Development of a 50-kW, low-emission turbo-generator for hybrid electric vehicles", ASME paper 98-GT-400.

Pullen K.R., Baines N.C., Hill S.H. (1992) "The design and evaluation of a high pressure ratio radial turbine", ASME paper 92-GT-93.

Ray E.R., Ruby J.D. (1992) "Evaluation of the Westinghouse Solid Oxide Fuel Cell technology for electric utility applications in Japan", EPRI TR-100713,1992.

Singhal S.C. (1997) "Recent progress in tubular SOFC technology", proc. of the V Int. Symposium on Solid oxide fuel cells (SOFC-V), Vol. 97-40, The Electrochemical Society Inc. , NJ 1997.

Stephenson D., Ritchey I. (1997) "Parametric study of fuel cell and gas turbine combined cycle performance", ASME paper 97-GT-340.

Uchida H., Shiraki m., Bessho A., Yagi Y. (1994) "Development of a centrifugal compressor for 100 kW automotive ceramic gas turbine", ASME paper 94-GT-73.

Veyo S. (1996) "The Westinghouse SOFC program - a status report", proc. of the 31st IECEC, n.96570, pp. 1138, 1996.

Veyo S. and Forbes C. (1998) "Demonstrations based on Westinghouse's prototype commercial AES design ", proc. of the Third European Solid Oxide Fuel Cell Forum, pp.79-86, 1998.